Analyst

ROYAL SOCIETY OF CHEMISTRY

COMMUNICATION

View Article Online
View Journal | View Issue

Cite this: *Analyst*, 2022, **147**, 4724

Received 23rd August 2022,
Accepted 28th September 2022

DOI: 10.1039/d2an01390h

rsc.li/analyst

Nitric acid concentration strongly influences low level uranium determination on PEDOT-PSS coated glassy carbon electrodes†

Rahul Agarwal, *[a,b] Rama Mohana Rao Dumpala [c,d] and Manoj K. Sharma[a,b]

Understanding the parametric optimization and addition of modifications in existing techniques are the keys to successful research in the analytical sciences. The present study reports an electroanalytical technique by modifying an electrode with PEDOT-PSS and adjusting the analyte solution to lower acidity (0.05 M) levels. The proposed methodology achieved a detection limit of 1.24 ppb of uranium, which is far below the available concentrations of uranium in seawater; the WHO permissible limit for uranium in drinking water; and the allowed disposal limit for uranium in radioactive waste solutions. Redox characteristics and speciation analysis supported by theoretical prediction helped to understand the basic mechanism which lay behind the achievement of such low detection limits. The technique was successfully employed for uranium determination in real water samples and the results were validated by another independent technique (ICP-MS).

Uranium is the most studied actinide element owing its extensive usage as a nuclear fuel material. The progress of nuclear energy is always associated with the challenges of handling, containing and concealing the radioactivity prior, during and after reactor operations. Uranium, being both a radiochemical and biological hazard, necessitates restricted release and high confinements. The concentration of uranium present or that could disposed of depends on the primary source.[1,2] U ore reserves on land (~4.5 million tons) are scarce but abundant in sea water (~1000 times those on land), and this can be a rich U resource if we are able to efficiently extract U from sea water. However, selective extraction of U from sea water is highly challenging owing to the ultralow of U concentration in sea water (3.3 ppb).[3,4] Thus it is of great importance to develop a sensitive method for trace level determination of U, to limit its exposure to aquatic and biological environments, for the selective extraction of U for the use of U as nuclear fuel in nuclear reactors, as well as to check that nuclear effluents to fall below the disposal limits. α-Spectroscopy,[5,6] neutron activation analysis,[7,8] and inductively coupled mass spectrometry[9,10] are commonly employed to determine U at trace and ultra-trace levels. But these techniques are limited by their high-cost, requirements for specialized personnel, and non-portability outside of sophisticated laboratories. The electrochemical method with all these advantages offers a good choice for developing an analytical procedure to detect uranium.[11] Stripping voltammetry attains lower detection limits among the electroanalytical techniques owing to the added advantage of pre-concentration on the electrode prior to determination.

Poly(3,4-ethylenedioxythiophene)-poly(styrenesulfonate) (PEDOT-PSS) is a widely used conducting polymer for the preparation of low-cost chemically-modified electrodes because of its high stability, aqueous processability, low cost, and high electrical conductivity.[12] PEDOT is water-insoluble and for aqueous processability, it is doped with the surfactant PSS.[13] Herein, we report the very low level of U determination down to ppb level using cathodic stripping voltammetry (CSV) using a PEDOT-PSS/glassy carbon (PEDOT-PSS/GC) electrode in aqueous medium. At first, the electrochemistry of U was explored in nitric acid using a PEDOT-PSS/GC electrode and it was observed that the height of the U(VI) to U(IV) reduction peak increases with decreases in nitric acid concentration.‡ Energy Dispersive Spectroscopy (EDS), a speciation study and Density Functional Theory (DFT) was used to understand the mechanism responsible for such nitric acid concentration dependence of the electrochemical response of the U(VI) to U(IV) reduction peak on the PEDOT-PSS/GC electrode. The large peak heights of the U(VI) to U(IV) reduction peak at low

[a]*Homi Bhabha National Institute, Mumbai 400 094, India.*
E-mail: rahulmarru@barc.gov.in, rahulagarwal715@gmail.com;
Fax: +91 22 2550 5151; Tel: +9122 2559 0642
[b]*Fuel Chemistry Division, Bhabha Atomic Research Centre (BARC), Trombay, Mumbai 400 085, India*
[c]*Radiochemistry Division, Bhabha Atomic Research Centre (BARC), Trombay, Mumbai 400085, India*
[d]*Institute for Nuclear Waste Disposal, Karlsruhe Institute of Technology, P.O. Box 3640, 76021 Karlsruhe, Germany*

† Electronic supplementary information (ESI) available. See DOI: https://doi.org/10.1039/d2an01390h

nitric acid molarity has analytical importance. Linear sweep voltammetry (LSV) results show a drastic improvement in the detection limit for U is observed with lowering the nitric acid concentration which facilitates more UO_2^{2+} ion adsorption on PEDOT-PSS and 0.05 M HNO_3 is the preferred choice for trace level U determination in aqueous medium. To bring down the detection limit for U determination even further, the dual advantage of 0.05 M HNO_3 is utilized in which the adsorbed UO_2^{2+} is electrochemically reduced to water insoluble UO_2 which precipitates and pre-concentrates U at the PEDOT-PSS/GC electrode surface. Eventually, a detection limit of as low as 1.24 ppb of U was achieved using cathodic stripping voltammetry (CSV). The present methodology is evaluated with a real water sample and the results are also validated with inductively coupled plasma mass spectrometry (ICP-MS).

LSVs of 0.5 mM UO_2^{2+} in 1 M HNO_3 using (i) GC and (ii) PEDOT-PSS/GC electrodes been recorded (Fig. 1a); wherein GC showed a cathodic peak at −0.330 V with a peak current density of 51.7 μA cm^{-2} ('i' in Fig. 1a) which corresponds to the reduction of UO_2^{2+} to U^{4+}. The reduction proceeds through conversion of UO_2^{2+} to UO_2^{+} (eqn (1)); and the instantaneous disproportionation of UO_2^{+} into UO_2^{2+} and U^{4+} (eqn (2)).[14,15] Thus, all UO_2^{2+} reduces into U^{4+} at −0.330 V as a result of fast disproportionation of UO_2^{+} in an acidic medium (eqn (3)).

$$2UO_2^{2+} + 2e^- = 2UO_2^{+} \quad (1)$$

$$2UO_2^{+} + 4H^+ = UO_2^{2+} + U^{4+} + 2H_2O \quad (2)$$

$$UO_2^{2+} + 4H^+ + 2e^- = U^{4+} + 2H_2O \quad (3)$$

The modification of the GC electrode by PEDOT-PSS shifted the UO_2^{2+} to U^{4+} reduction peak to −0.174 V with an increased peak-current density (−112.5 μA cm^{-2}) ('ii' in Fig. 1a). Thus, the energy barrier for electron transfer between the electrode and UO_2^{2+} centres is significantly reduced at PEDOT-PSS and shows enhanced electrochemical response as compared to GC.[15] The electrochemical response for UO_2^{2+} reduction at both GC and PEDOT-PSS/GC followed a linear variation in peak current with square root of scan rate ($\sqrt{\vartheta}$) (Fig. S3 and S4†) and had slopes for $\ln(j_P^c)$ (j_P^c = cathodic peak-current

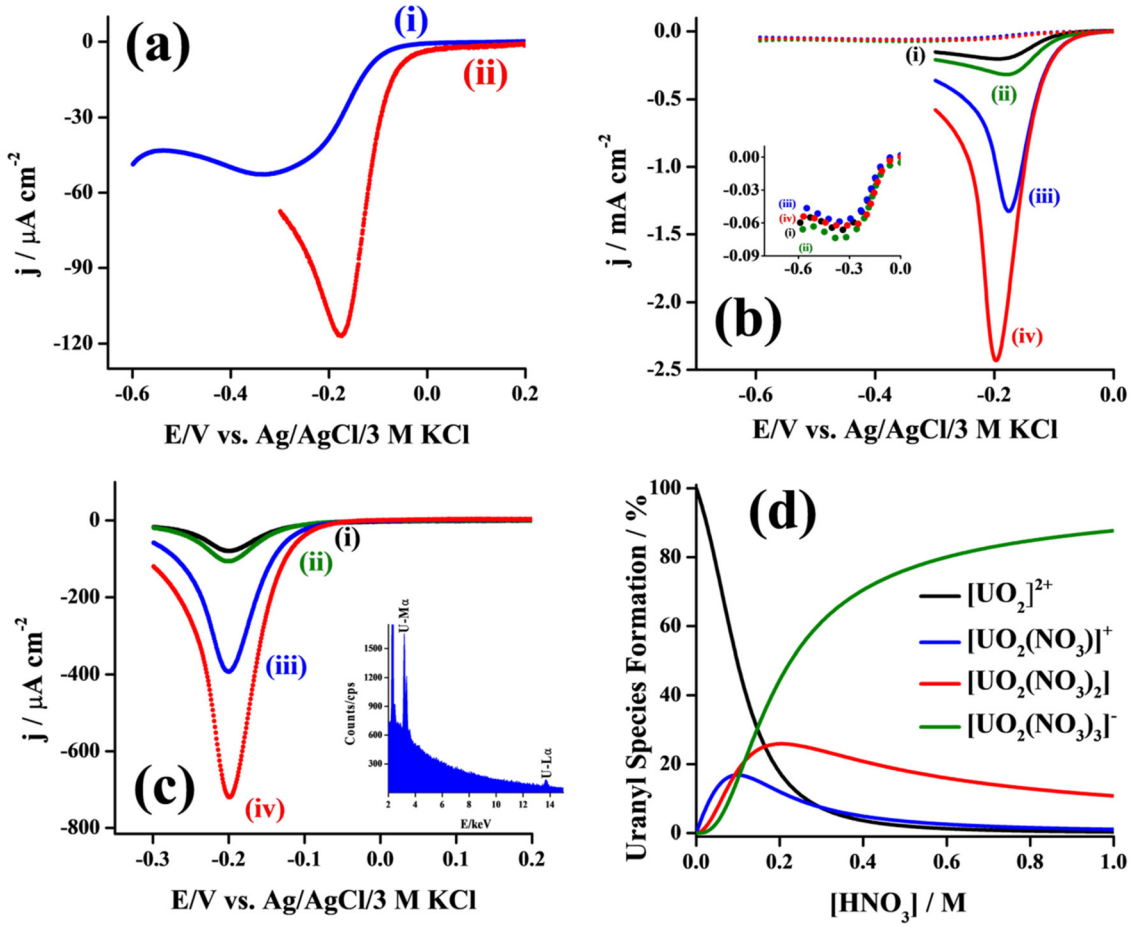

Fig. 1 (a) LSVs of 0.5 mM UO_2^{2+} in 1 M HNO_3 using (i) GC (blue line) and (ii) PEDOT-PSS/GC (red line) at a scan rate of 50 mV s^{-1}. (b) LSVs of 0.5 mM UO_2^{2+} using GC (dotted line) and PEDOT-PSS/GC (solid line) at a scan rate of 100 mV s^{-1} at different acid strengths ((i) 1 M, (ii) 0.5 M, (iii) 0.1 M and (iv) 0.05 M HNO_3). Inset shows the zoomed portion of GC electrode. (c) LSVs of PEDOT-PSS/GC electrode in 0.05 M HNO_3 at a scan rate of 100 mV s^{-1} after dipping the electrode in 0.5 mM UO_2^{2+} in (i) 1 M; (ii) 0.5 M; (iii) 0.1 M and; (iv) 0.05 M HNO_3, respectively for 10 minutes. Inset shows the EDS spectra of PEDOT-PSS/GC electrode after UO_2^{2+} adsorption. (d) Species distribution of UO_2^{2+} with variation in HNO_3 acid concentration.

density) *versus* ln(ϑ) of 0.36 for GC, and 0.43 for PEDOT-PSS/GC, indicating a purely diffusion controlled process for UO_2^{2+} reduction at both the electrodes. LSVs of 0.5 mM UO_2^{2+} at various acid strengths of HNO_3 (1 M to 0.05 M) using both GC (dotted line in Fig. 1b) and PEDOT-PSS/GC (solid line in Fig. 1b) electrodes at a scan rate of 100 mV s^{-1} were recorded to find out the effect of pH on the UO_2^{2+}/U^{4+} couple. The peak current density of U(VI) to U(IV) reduction is constant on GC but increases drastically on PEDOT-PSS/GC with a decrease in acid strength (concentration of HNO_3). To get more insight, four different PEDOT-PSS/GC electrodes were dipped in 0.5 mM UO_2^{2+} in 1 M, 0.5 M, 0.1 M and 0.05 M HNO_3, respectively for 10 minutes, washed several times with Milli-Q water and then the LSV of each electrode was recorded in blank solution (0.05 M HNO_3) at a scan rate of 100 mV s^{-1} (Fig. 1c). A reduction peak at −0.172 V was observed in each case which signifies uranyl ion adsorption on PEDOT-PSS.[16] But the height of the U(VI) to U(IV) reduction peak current is greater at lower acidity (0.05 M HNO_3) which signifies the amount of UO_2^{2+} ions adsorption on PEDOT-PSS/GC electrodes increases with a decrease in nitric acid strength. The same experiment was performed with bare GC electrode but no adsorption of UO_2^{2+} was observed. To further confirm uranyl adsorption on PEDOT-PSS, the PEDOT-PSS/GC electrode was dipped in 0.1 M UO_2^{2+} in 0.05 M HNO_3 overnight, washed several times with Milli-Q water and the EDS spectrum of the electrode was recorded (inset of Fig. 1c). The EDS spectrum confirms UO_2^{2+} adsorption on PEDOT-PSS. Because of the UO_2^{2+} adsorption, the energy barrier for electron transfer between the electrode and UO_2^{2+} centres is significantly reduced at PEDOT-PSS and shows enhanced electrochemical response as compared to GC (Fig. 1a).

Speciation analysis depicting the percentage of free and complexed uranyl ions present in solution with variation in acid concentration (Fig. 1d) would be a useful tool to interpret the observation of high peak current densities at lower acidity. UO_2^{2+} ions get adsorbed on the surface of PEDOT-PSS/GC due to interaction with negatively charged PSS^-.[17–20] UO_2^{2+} is expected to form $[UO_2(NO_3)]^+$, $[UO_2(NO_3)_2]$ and $[UO_2(NO_3)_3]^-$ species in solution. Thus, the free UO_2^{2+} and $[UO_2(NO_3)]^+$ species possess high electrostatic attraction for PSS^- anions, while $[UO_2(NO_3)_2]$ and $[UO_2(NO_3)_3]^-$ species would be non-interacting with PSS^- anions and would remain in solution rather than getting adsorbed on the electrode. The speciation plot (Fig. 1d) shows that at lower acidity (0.05 M) UO_2^{2+} (~77%) and $[UO_2(NO_3)]^+$ (~13%) are the dominant species, while at higher acidity (>0.3 M), $[UO_2(NO_3)_2]$ and $[UO_2(NO_3)_3]^-$ species amount to ~24% and ~61% of the species formation respectively. Thus, the lower acidity allows more UO_2^{2+} ions to get adsorbed on PEDOT-PSS/GC electrode, while the increase in acidity facilitates the formation of non-adsorbing $[UO_2(NO_3)_2]$ and $[UO_2(NO_3)_3]^-$ species, and thereby decreasing the peak current densities and hence the sensitivity (Fig. 1b).

A molecular-level understanding of the interaction of different species with the same substrate could shed light on key factors (energetics, bond distances, partial charges) responsible for the differential binding of one species over another. Zotti *et al.* experimentally showed that a trimer of PEDOT possesses a mono-positive charge and PSS in mono-negative form interacts with PEDOT radical ions.[21] Thus, the present studies also employed the trimer units of PEDOT and PSS for optimization of PEDOT-PSS structures initially. UO_2^{2+} is expected to form $[UO_2(NO_3)]^+$, $[UO_2(NO_3)_2]$ and $[UO_2(NO_3)_3]^-$ species in solution depending on the concentration of HNO_3. Thus, the optimized geometry was configured with UO_2^{2+} and its nitrate species on the other ends of the PSS moiety for geometry optimization of PEDOT-PSS-UO_2^{2+}-NO_3 species. Geometry optimization by the combination of B3-LYP functional and def-SVP basis set followed by energetics calculations using the def-TZVP basis set using density functional theory (DFT) was found to be appropriate to interpret the uranyl speciation at molecular level.[22–24] Thus, the present studies also employed a similar protocol for geometry optimization and energetics estimation of PEDOT, PSS, PEDOT-PSS, PEDOT-PSS-UO_2^{2+}, and PEDOT-PSS-$UO_2(NO_3)$, PEDOT-PSS-$UO_2(NO_3)_2$, PEDOT-PSS-$UO_2(NO_3)_3$ species. Two C–O bonds formed by carbon atoms common to dioxy and thiophene rings in the centre monomer of the PEDOT trimer with the two oxygen atoms of sulphonate group of PSS, and an intermolecular hydrogen bonding (O–H) between hydrogen of CH_2 from PEDOT and the third oxygen of PSS group results in the formation of the PEDOT-PSS species (Fig. 2). The sulphonate group on the opposite end to the PEDOT edge in PEDOT-PSS is attached with $UO_2^{2+}/UO_2(NO_3)/UO_2(NO_3)_2/UO_2(NO_3)_3$ for geometry optimization of PEDOT-PSS-UO_2^{2+}/its nitrate species. The binding energies as well as Gibbs free energies for the formation of PEDOT-PSS-UO_2^{2+} species were found to be more negative than PEDOT-PSS-UO_2^{2+}-nitrate species. Relatively more negative values (Table T1, ESI†) indicate the preferential binding of UO_2^{2+} to PEDOT-PSS over its nitrate species and the same is attributed to the experimentally observed higher peak currents for UO_2^{2+} at lower HNO_3 concentrations (Fig. 1b). Further, to gain deeper insights, the bond distances and partial charges on binding moieties were also estimated using DFT at TZVP level. U and its nitrate species interact through the PSS moiety at the sulphonate group by U–O bond formation in the PEDOT-PSS interface. The calculated bond distances for the U–O bond are found to be shorter in PEDOT-PSS-UO_2 (2.21 Å, 2.22 Å) compared to PEDOT-PSS-$UO_2(NO_3)$ (2.38 Å, 2.39 Å) and PEDOT-PSS-$UO_2(NO_3)_2$ (2.51 Å, 2.51 Å), while in PEDOT-PSS-$UO_2(NO_3)_3$, uranium binds through the single oxygen of sulphonate group, further affirming the preferential binding for UO_2^{2+} over its nitrate species by PEDOT-PSS.

The enhanced peak current of U(VI) to U(IV) reduction at lower nitric acid concentration signifies the analytical importance of the PEDOT-PSS/GC electrode for the determination of U at trace levels. Peak current densities measured by LSV at PEDOT-PSS/GC electrode showed a linear relation with UO_2^{2+} concentration at two different acidities (1 & 0.05 M HNO_3; Fig. 3a & b). The limit of detection (LOD) of U on PEDOT-PSS/GC was estimated to be 9.97 and 0.32 μM in 1 and 0.05 M

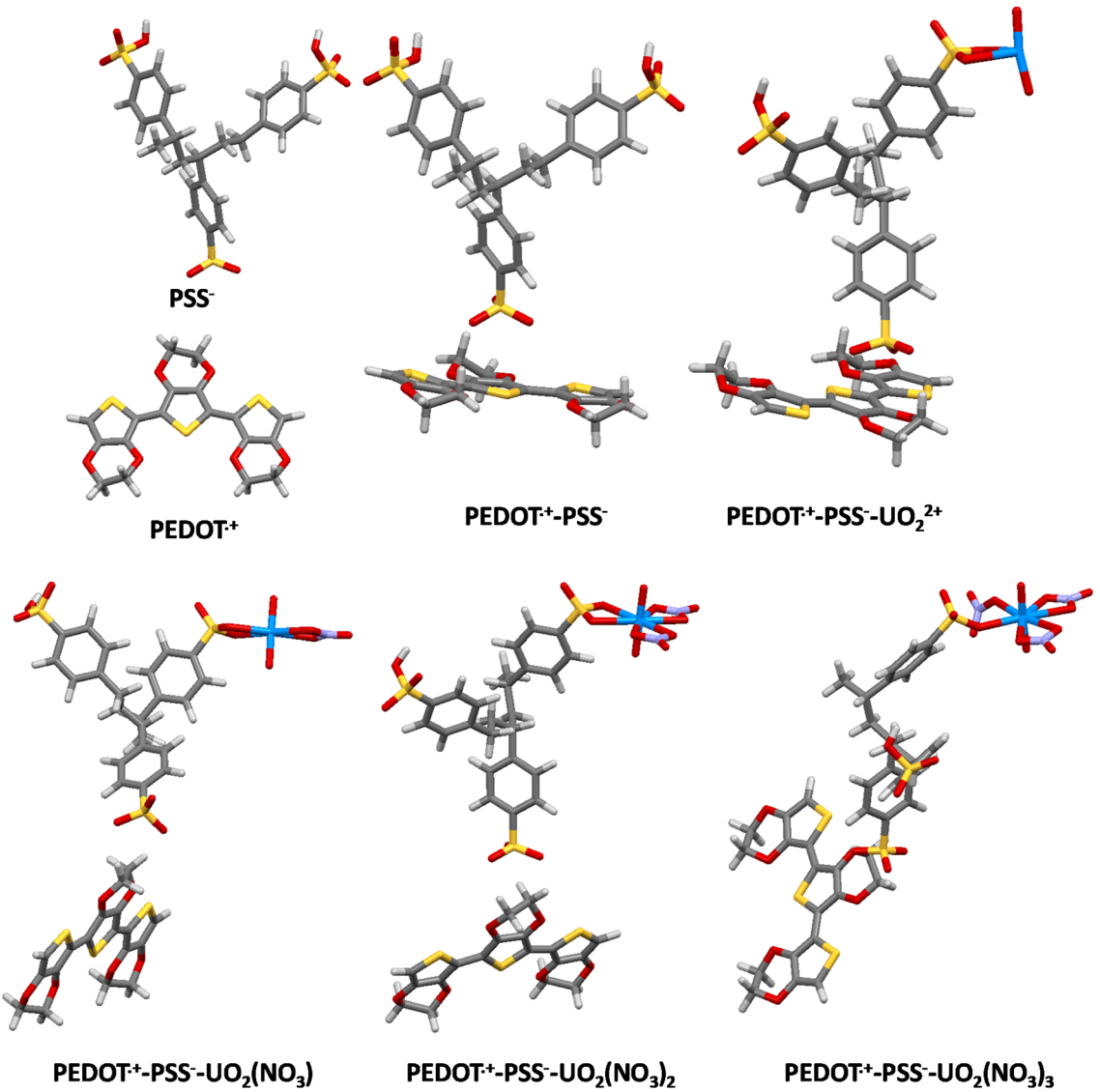

Fig. 2 Optimized geometries for PEDOT, PSS, PEDOT-PSS, PEDOT-PSS-UO_2, PEDOT-PSS-$UO_2(NO_3)$, PEDOT-PSS-$UO_2(NO_3)_2$, PEDOT-PSS-$UO_2(NO_3)_3$ species. Colour code: yellow – sulfur (S), red – oxygen (O), grey – carbon (C), white – hydrogen (H), blue – uranium (U).

HNO_3, respectively. The improvement in LOD of U in 0.05 M HNO_3 on PEDOT-PSS is ascribed to more UO_2^{2+} adsorption on PEDOT-PSS at lower acidity which results in an enhancement in the peak-current density. The LOD of U was also determined on bare GC electrode and is found to be 10 μM of U irrespective of acid strength (Fig. S5†). Therefore, PEDOT-PSS/GC as the electrode and 0.05 M HNO_3 as the solution medium are ideal choices for U determination at low levels. Besides, 0.05 M HNO_3 as the solution medium has dual advantages. It not only results in more UO_2^{2+} adsorption on PEDOT-PSS but electrochemical reduction of the adsorbed UO_2^{2+} in 0.05 M HNO_3 results in formation of neutral UO_2 which is water insoluble and precipitates on the electrode surface. But the same in 1 M HNO_3 results in the formation of water soluble U^{4+} which diffuses away from the electrode surface.[1,25] This can be further exploited as an efficient tool to pre-concentrate U as UO_2 on the electrode surface by applying a constant negative potential (−0.3 V) followed by scanning towards negative potentials which results higher reduction currents. Hence, Cathodic Stripping Voltammetry (CSV) is exploited to further improve the LOD of U in 0.05 M HNO_3 on PEDOT-PSS/GC. Fig. 3c shows the CSVs of 1 μM UO_2^{2+} (i) without and (ii) with pre-concentration of UO_2 at a fixed deposition potential (−0.3 V) for 180 s which shows an enhancement in peak-current density of the UO_2^{2+} to UO_2 reduction peak. Next, CSVs of 1 μM UO_2^{2+} were recorded for different deposition times at a constant negative potential of −0.3 V (Fig. 3d). They show a linear correlation of peak-current density *versus* deposition time. More UO_2 gets precipitated at the electrode surface as deposition time increases and this results in a higher peak current. CSVs of different concentrations of UO_2^{2+} were recorded at a fixed deposition potential of −0.3 V for 300 s

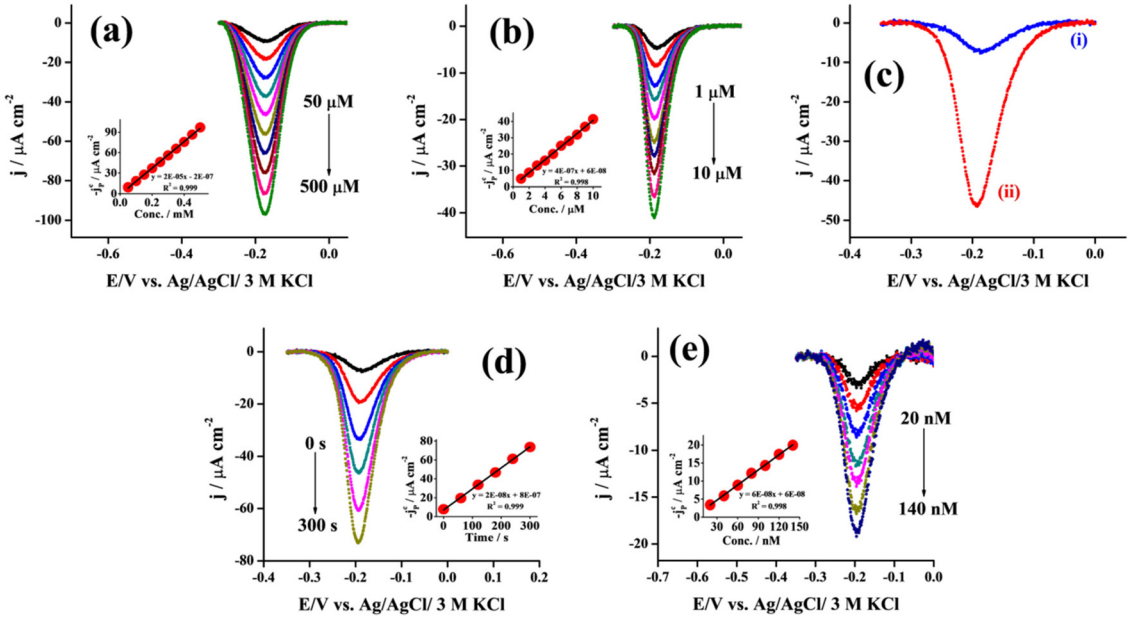

Fig. 3 LSVs of different concentrations of UO_2^{2+} in (a) 1 M HNO_3 and (b) 0.05 HNO_3 using a PEDOT-PSS/GC electrode at a scan rate of 100 mV s^{-1}. Insets show the plot of peak-current density *versus* U concentration. CSVs of PEDOT-PSS/GC electrode in (c) 1 μM UO_2^{2+} in 0.05 M HNO_3 (i) without and (i) with pre-concentration of UO_2 at a fixed deposition potential (−0.3 V) for 180 s; (d) 1 μM UO_2^{2+} in 0.05 M HNO_3 at a fixed deposition potential (−0.3 V) for different deposition times; inset shows the plot of peak-current density *versus* deposition time; (e) different concentrations of UO_2^{2+} in 0.05 HNO_3 at a fixed deposition potential (−0.3 V) for 300 s. Inset shows the plot of peak-current density *versus* U concentration. All the CSVs are recorded at a scan rate of 100 mV s^{-1}.

using PEDOT-PSS/GC electrode (Fig. 3e), and it was observed that the peak-current density increases linearly with increase in U concentration. The LOD of U was found to be 5.21 nM (1.24 ppb) of U. The present methodology was tested to quantify U in a real water sample obtained from the Municipal Corporation of Greater Mumbai (MCGM). The water molarity was adjusted to 0.05 M HNO_3 and U was not detected in MCGM supplied water and so it is spiked with a known quantity of UO_2^{2+} (20 nM). Initially, CSVs of the spiked water were recorded followed by standard solutions of UO_2^{2+} in 0.05 M HNO_3 of varying concentrations. A linear correlation of peak currents *versus* U concentration was obtained. The amount of U present in spiked water is determined as 19.24 ± 0.19 nM (repeatable measurements, n = 3). The same sample was tested with ICP-MS and concentration of U was found out to be 19.36 ± 0.12 nM.

The electrochemical response of the PEDOT-PSS/GC in UO_2^{2+} in 0.05 M HNO_3 is found to be repeatable, reproducible and stable (Fig. S6–S8†) and also free from the interference of other metal ions (Na^+, K^+, NH_4^+, Ba^{2+}, Cd^{2+}, Co^{2+}, Cu^{2+}, Hg^{2+}, Mg^{2+}, Mn^{2+}, Ni^{2+}, Pb^{2+}, Zn^{2+} and Fe^{3+}) present in aqueous medium (Fig. S9†).

In summary, the crucial role of nitric acid concentration for determining very low levels of U on a PEDOT-PSS/GC electrode is discussed in the manuscript. LSV, speciation and DFT studies shows that the preferential binding of free UO_2^{2+} to PEDOT-PSS over its nitrate species ($[UO_2(NO_3)]^+$, $[UO_2(NO_3)_2]$ and $[UO_2(NO_3)_3]^-$) in low nitric acid strength is the main reason for obtaining very low detection limits for UO_2^{2+} on a PEDOT-PSS coated GC electrode. The insolubility of UO_2 in 0.05 M HNO_3 is an added advantage to bring the LOD of U down to the ppb level.

Author contributions

Rahul Agarwal: conceptualization, data curation, formal analysis, investigation, methodology, resources, validation, writing – original draft, writing – review & editing; Rama Mohana Rao Dumpala: data curation, methodology, validation, writing – review & editing and Manoj K Sharma: resources and supervision.

Conflicts of interest

The authors declare no competing financial interest.

Acknowledgements

Our institute is a government funded research institute, so, financial support is from BARC, Government of India. The authors wish to thank Dr S. Kannan and Dr Renu Agarwal, FCD, BARC for their constant support and encouragement in this work.

References

‡ ^{238}U ($t_{1/2}$ = 4.5 × 10^9 years) is a α-emitting radionuclide and hazardous. Due to its radiological and chemical toxicity, it should be handled in fume hoods and glove boxes in dedicated radioactive laboratories by trained personnel.

1 Y. Peled, E. Krent, N. Tal, H. Tobias and D. Mandler, *Anal. Chem.*, 2015, **87**, 768–776.
2 S. K. Guin, A. S. Ambolikar, J. P. Guin and S. Neogy, *Sens. Actuators, B*, 2018, **272**, 559–573.
3 X. Liu, Y. Xie, M. Hao, Z. Chen, H. Yang, G. I. Waterhouse, S. Ma and X. Wang, *Adv. Sci.*, 2022, **9**, 2201735.
4 M. Hao, Z. Chen, X. Liu, X. Liu, J. Zhang, H. Yang, G. I. Waterhouse, X. Wang and S. Ma, *CCS Chem.*, 2022, 1–14.
5 M. J. Vargas, A. M. Sanchez and F. V. Tomé, *Nucl. Instrum. Methods Phys. Res., Sect. A*, 1994, **346**, 298–305.
6 R. Weber, R. Esterlund and P. Patzelt, *Appl. Radiat. Isot.*, 1999, **50**, 929–934.
7 A. R. Byrne and L. Benedik, *Anal. Chem.*, 1997, **69**, 996–999.
8 L. Zikovsky, *J. Radioanal. Nucl. Chem.*, 2004, **260**, 219–220.
9 P. Grinberg, S. Willie and R. E. Sturgeon, *Anal. Chem.*, 2005, **77**, 2432–2436.
10 S. Joannon, P. Telouk and C. Pin, *Spectrochim. Acta, Part B*, 1997, **52**, 1783–1789.
11 R. Gupta, M. Sundararajan and J. S. Gamare, *Anal. Chem.*, 2017, **89**, 8156–8161.
12 P. P. Cottis, D. Evans, M. Fabretto, S. Pering, P. Murphy and P. Hojati-Talemi, *RSC Adv.*, 2014, **4**, 9819–9824.
13 L. Qin, Q. Tao, A. El Ghazaly, J. Fernandez-Rodriguez, P. O. Persson, J. Rosen and F. Zhang, *Adv. Funct. Mater.*, 2018, **28**, 1703808.
14 D. Kabir ud, J. Kůta and L. Pospisil, *Electrochim. Acta*, 1977, **22**, 1109–1112.
15 S. K. Guin, K. Parvathi, A. S. Ambolikar, J. S. Pillai, D. K. Maity, S. Kannan and S. K. Aggarwal, *Electrochim. Acta*, 2015, **154**, 413–420.
16 M. K. Sharma, A. S. Ambolikar and S. K. Aggarwal, *Radiochim. Acta*, 2011, **99**, 555–562.
17 M. Zhang, W. Yuan, B. Yao, C. Li and G. Shi, *ACS Appl. Mater. Interfaces*, 2014, **6**, 3587–3593.
18 K. Woon, W. Wong, N. Chanlek, H. Nakajima, S. Tunmee, V. Lee, A. Ariffin and P. Songsiriritthigul, *RSC Adv.*, 2020, **10**, 17673–17680.
19 L. Yan, X. Gao, J. P. Thomas, J. Ngai, H. Altounian, K. T. Leung, Y. Meng and Y. Li, *Sustainable Energy Fuels*, 2018, **2**, 1574–1581.
20 S. H. Lee, J. H. Bang, J. Kim, C. Park, M. S. Choi, A. Mirzaei, S. S. Im, H. Ahn and H. W. Kim, *Sens. Actuators, B*, 2021, **327**, 128924.
21 G. Zotti, S. Zecchin, G. Schiavon, F. Louwet, L. Groenendaal, X. Crispin, W. Osikowicz, W. Salaneck and M. Fahlman, *Macromolecules*, 2003, **36**, 3337–3344.
22 R. M. R. Dumpala, A. Boda, A. Srivastava, P. Kumar, N. Rawat and S. M. Ali, *Chemosphere*, 2020, **249**, 126116.
23 R. M. R. Dumpala, S. K. Das, M. Ali, A. Boda, P. Kumar, N. Rawat, A. Kumar and S. M. Ali, *Chemosphere*, 2021, **271**, 129547.
24 S. Sharma, R. M. R. Dumpalan and N. Rawat, *Inorg. Chim. Acta*, 2020, **508**, 119653.
25 T. Cordara, S. Szenknect, L. Claparede, R. Podor, A. Mesbah, C. Lavalette and N. Dacheux, *J. Nucl. Mater.*, 2017, **496**, 251–264.